Applied Science, Computing and Energy, 2026, 4(2), 217-232

Fe (III) and Ni (II) Nano Complexes of Metronidazole; Synthesis, Characterisation, and Antioxidant Studies

Chimuanya Benjamin Okezie, Lord Okechukwu C. Ubani, Brendan Chidozie Asogwa, Ifeanyi Edozie Otuokere, and Chigozie Mbara

17 September 2025/Accepted: 12 March 2026 /Published: 30 March 2026

Abstract: *Metronidazole (MTZ), a nitroimidazole antibiotic widely used for the treatment of anaerobic bacterial and protozoal infections, is increasingly limited by reduced efficacy, toxicity concerns, and emerging microbial resistance. In this study, nano-sized Fe(III) and Ni(II) complexes of MTZ were synthesized via a sonochemical method and characterized using UV–Visible, FTIR, and ^{1}H NMR spectroscopic techniques, alongside morphological analysis. The complexes were obtained in high yields of 89% for [Fe(MTZ)$_2$] and 80% for [Ni(MTZ)$_2$], with distinct colour changes (black and blue, respectively) and melting points of 157 °C and 200 °C, compared to 160 °C for free MTZ, confirming complex formation. FTIR analysis revealed shifts in key vibrational bands, including O–H stretching from 3204 cm^{-1} to 3190 cm^{-1} (Ni complex) and its disappearance in the Fe complex, indicating deprotonation, while the C=N band shifted from 1530 cm^{-1} to 1521–1517 cm^{-1}, confirming coordination through the imidazole nitrogen. ^{1}H NMR spectra showed corresponding changes, including disappearance of the hydroxyl proton in the Fe(III) complex and slight shifts in aromatic and methyl proton signals. UV–Visible spectra exhibited ligand-centered $\pi \rightarrow \pi^*$ transitions at 257 nm shifting to 260 nm (Fe) and 242 nm (Ni), with additional weak d–d transition observed at ~794 nm for the Fe(III) complex, consistent with an octahedral geometry. Transmission electron microscopy revealed nanoscale particles with sizes predominantly in the range of 2.70–5.32 nm, confirming successful nano-complex formation. Antioxidant evaluation using DPPH and FRAP assays showed negligible activity for both MTZ and its complexes, with absorbance values close to zero across concentrations of 25–400 µg mL^{-1}, indicating a lack of significant radical scavenging and reducing power. The results confirm the successful synthesis of nano-sized Fe(III) and Ni(II) metronidazole complexes with modified structural and physicochemical properties. However, these modifications do not translate into enhanced antioxidant activity, suggesting that the complexes may be better suited for applications in drug delivery and nanomedicine rather than as direct antioxidant agents.*

Keywords: *Metronidazole, Fe (III), Ni (II), antioxidant activity*

Chimuanya Benjamin Okezie
Department of Chemistry,
Federal University, Otuoke, Bayelsa State.
Email: chimokezie46@gmail.com

Ubani L. O. C.
Department of Chemistry,
Michael Okpara University of Agriculture,
Umudike, Abia State, Nigeria
Email: okechukwu.ubani@mouau.edu.ng

Brendan Chidozie Asogwa
Department of Chemistry,
Michael Okpara University of Agriculture,
Umudike, Abia State, Nigeria
Email: chidonwasogwa@gmail.com
https://orcid.org/0009-0009-8530-9982

Ifeanyi Edozie Otuokere
Department of Chemistry,
Michael Okpara University of Agriculture,
Abia, Nigeria.
Email: ifeanyiotuokere@gmail.com
https://orcid.org/0000-0003-0038-8132

Chigozie Mbara
Department of Chemistry,
Alvan Ikoku Federal University of Education,
Owerri, Imo State, Nigeria
Email: chigozie.mbara@alvanikoku.edu.ng

1.0 Introduction

The coordination of bioactive organic ligands with transition metals is a well-established strategy for modulating physicochemical properties, enhancing bioavailability, and introducing new pharmacological activities, including antioxidant potential. (Singh *et al*., 2012). This approach has become increasingly important as many therapeutic agents have become less effective in treating infections due to the growingchallenge of antibiotic resistance. "Antibiotic resistance arises from several factors, including misuse and overuse of drugs, extensive application of antibiotics in agriculture, and genetic mutations in microbial DNA. Consequently, the coordination of transition metals with existing drugs has shown significant potential as an alternative strategy for combating antibiotic resistance. Metronidazole (MTZ) is a widely used nitroimidazole-derived antibiotic and antiprotozoal compound. It exhibits high efficacy against anaerobic bacteria and protozoan parasites. (Löfmark *et al*., 2010). "The pharmacological activity of metronidazole arises from intracellular reduction of its nitro group.
of the microbe (Onyegbule *et al*., 2021). Despite its widespread clinical use, metronidazole exhibits limited physicochemical and biological versatility, with its activity largely restricted to nitro-reductive mechanisms and minimal reported antioxidant or redox-modulating properties. (Asogwa *et al.,* 2025). "These limitations, combined with the increasing prevalence of resistant microbial strains, have reduced its overall therapeutic effectiveness. (Nyah *et al.,* 2025).

Nano-sized metal complexes, in particular, offer advantages such as improved cellular uptake and potential for targeted delivery via the Enhanced Permeability and Retention (EPR) effect (Patra *et al*., 2018). One of the green and efficient approaches for synthesizing nano-sized compounds is the sonochemical method. This method involves the utilization of high-intensity ultrasound usually between 20kHz – 10 MHz to create bubbles that collapse to produce localized temperatures of approximately 5000 K and pressures exceeding 1000 atm, usually called acoustic cavitation (Asogwa *et al.,* 2024). Compounds produced via the sonochemical method are typically homogeneous and exhibit enhanced reactivity (Asogwa *et al.,* 2025). The use of sonochemical methods in synthesizing nano-sized particles created a new area of research in medicine where both known therapeutic compounds and novel compounds such as metal complexes of drugs are now being formulated in nano-sized particles to increase its bioavailability, solubility, stability and other physicochemical properties as thereby enhancing their applicability in targeted drug delivery and precision medicine (precision medicine).
However, despite advances in metallodrug development, there is limited information on the synthesis, characterization, and antioxidant evaluation of nano-sized metal complexes of metronidazole.
Iron (Fe) and nickel (Ni) are biologically relevant transition metals known to form stable complexes with nitrogen- and oxygen-donor ligandswith nitrogen- and oxygen-donor ligands, often influencing the redox behavior of the resulting compounds (El-Wahab *et al*., 2019; Nyah *et al.,* 2026; Asogwa *et al.,* 2025). Previous studies have shown that metal complexation can alter the electronic structure of ligands, potentially introducing radical scavenging or reducing activity absent in the free ligand (Refat *et al*., 2014). However, the antioxidant potential of metronidazole metal complexes remains largely unexplored. This study aims to synthesize and characterize nano-sized Fe(III) and Ni(II) complexes of

metronidazole and to evaluate their in vitro antioxidant potential using DPPH and FRAP assays. This study is significant as it advances the understanding of nano-scale

and provides insights into the potential application of metronidazole-based complexes in drug delivery systems and future therapeutic design.

2.0 Materials and Methods

2.1 Chemicals and Solvents

All reagents and solvents used were of analytical grade and obtained from Andhra Organics Limited. They were used without further purification.

2.2 Synthesis

The nano-sized metal complexes were synthesized following the procedure reported by Asogwa and Otuokere (2024) with slight modifications. . Exactly 20 mL each of 0.05 mol solutions of $FeCl_3.6H_2O$ and $NiSO_4.6H_2O$ was added to 20 mL of 0.1 mol metronidazole solution.. Each reaction mixture was stirred and subjected to ultrasonic irradiation using a probe operating at 24 kHz and 400 W at a controlled temperature of 50 °C for 30 minutes.”“The resulting mixtures were filtered using Whatman No. 1 filter paper.. The filtrates were subsequently dried in a desiccator at room temperature.The dried complexes were weighed to determine percentage yield and stored in properly labeled airtight containers.

The formation of the metal complexes is proposed as shown in Equations (1) and (2):)$FeCl_3 \cdot 6H_2O + 2C_6H_9N_3O_3 \rightarrow [Fe(C_6H_8N_3O_3)_2] + 6H_2O + Cl_2 + HCl$ (1)

$NiSO_4 \cdot 6H_2O + 2\ C_6H_9N_3O_3 \rightarrow [Ni(C_6H_9N_3O_3)_2] + H_2SO_4 + 5\ H_2O$ (2)

2.3 Characterization

The melting points of the synthesized compounds were determined using a Gallenkamp melting point apparatus. The solubility profiles were determined using solvents of varying polarity (n-hexane, ethanol, water, ethyl acetate, and dimethyl sulfoxide (DMSO)). The UV/Vis spectroscopic results were obtained using a UV-1800 series spectrophotometer. FTIR spectra were obtained using a PerkinElmer Spectrum BX FT-IR spectrophotometer. H and ^{13}C NMR spectra were recorded on a Bruker Avance spectrometer operating at 600 MHz at 25 °C and processed using Mnova software.

2.4 In vitro Antioxidant Method

2.4.1 DPPH photometric assay

The free radical scavenging activity of the compounds was evaluated using the DPPH assay following the method of Mensor *et al*. (2001), with ascorbic acid used as the reference standard (Iwalewa *et al*., 2008). . Different concentrations of the compounds (25, 50, 100, 200, and 400 µg mL^{-1}) were prepared by adding a 1 mL of 0.5 mM DPPH (in methanol) in a cuvette. “The mixtures were incubated in the dark at room temperature for 30 minutes and the absorbance measured at 517 nm. The experiment was done in triplicate. The percentage antioxidant activities were calculated using equation 3

$$\% \text{ antioxidant activity (AA)} = \frac{Abs\ control - (Abs\ sample - Abs\ blank)}{Abs\ control} \times \frac{100}{1} \quad (3)$$

2.4.2 *FRAP*

The ferric reducing antioxidant power (FRAP) assay was performed according to the method described by Benzie and Strain (1999).. The FRAP reagent was prepared by mixing Acetate buffer, 2, 4, 6-triphridyl-s-triazine (TPTZ) and $FeCl_3\ 6H_2O$ in the ratio of 10:1:1, respectively. The FRAP reagent (3 mL) and 100 µl sample solution at concentrations of 25, 50, 100, 200 and 400 µg/mL were mixed and allowed to stand for 4 minutes. The absorbance of each mixture was recorded at 593 nm, at 37°C. The standard (ascorbic acid) was tested in a parallel process. The absorbance of each test tube was taken at 0 and 4 minutes after the addition of the sample. The FRAP value was calculated using equation 4

$$FRAP = abs(abs(4\ \text{min}) - abs(0\ min) \quad (4)$$

3.0 Results and Discussion

3.1 Physical Properties

The physical properties of metronidazole (MTZ) and its metal complexes are presented in Table 1. The free ligand appears as a white solid with a melting point of 160 °C, whereas the synthesized complexes exhibit distinct colour changes, appearing black for the Fe(III) complex and blue for the Ni(II) complex. These noticeable changes in colour, accompanied by the formation of precipitates during synthesis, provide preliminary evidence of successful coordination between the metal ions and the ligand. Such colour variations are characteristic of transition metal complexes and arise from electronic transitions within partially filled d-orbitals of Fe(III) and Ni(II), which alter the ligand field environment upon coordination (Asogwa *et al*., 2024).

Table 1: Physical Properties

Compounds	Colour	MP (°C)	% Yield
MTZ	White	160	-
[Fe(MTZ)$_2$]	Black	157	89
[Ni(MTZ)$_2$]	Blue	200	80

The melting point data further support complex formation. The Fe(III) complex shows a slight decrease in melting point (157 °C) compared to MTZ, suggesting a modification of intermolecular interactions due to coordination. In contrast, the Ni(II) complex exhibits a significantly higher melting point (200 °C), indicating the formation of a more thermally stable structure, possibly due to stronger metal–ligand interactions or a more rigid coordination framework. The relatively high percentage yields of 89% for [Fe(MTZ)$_2$] and 80% for [Ni(MTZ)$_2$] demonstrate the efficiency of the sonochemical synthesis method employed. From a technical perspective, the observed changes in colour and thermal properties confirm the formation of new coordination compounds with altered electronic and structural characteristics. The enhanced thermal stability, particularly in the Ni(II) complex, suggests potential suitability for applications requiring materials with improved stability under varying conditions.

3.2 *Solubility*

The solubility profiles of MTZ and its metal complexes in solvents of varying polarity are presented in Table 2. The free ligand (MTZ) shows limited solubility in non-polar n-hexane (insoluble) but is soluble or slightly soluble in polar solvents such as ethanol, ethyl acetate, water, and DMSO. Upon complexation, noticeable changes in solubility behaviour are observed, indicating the formation of new chemical species with modified intermolecular interactions.

The Fe(III) complex exhibits slight solubility in n-hexane and remains soluble in distilled water and DMSO, while showing reduced solubility in moderately polar solvents such as ethanol and ethyl acetate. Similarly, the Ni(II) complex is insoluble in n-hexane but soluble in water and DMSO, with slight solubility in ethanol and ethyl acetate. These variations suggest that coordination alters the overall polarity and solvation characteristics of the ligand.

The increased solubility of both complexes in highly polar solvents such as water and DMSO can be attributed to enhanced polarity arising from metal coordination, which promotes stronger interactions with polar solvent molecules (Otuokere *et al*., 2019). However, the limited solubility in non-polar solvents indicates that the complexes retain predominantly polar characteristics despite structural modification. The slight solubility of the Fe(III) complex in n-hexane may reflect subtle differences in molecular packing or surface interactions compared to the Ni(II) complex.

Technically, these solubility changes are significant, as they influence the handling, processing, and potential application of the complexes. Improved solubility in polar media suggests suitability for biological and pharmaceutical environments, where aqueous

compatibility is essential. Furthermore, the altered solubility behaviour supports the conclusion that coordination has significantly modified the physicochemical properties of metronidazole, reinforcing evidence for successful complex formation.

Table 2: Solubility Profile

Compounds	n-hexane	Distilled water	Ethanol	Ethyl Acetate	DMSO
MTZ	IS	SS	S	S	S
[Fe(MTZ)]	SS	S	SS	SS	S
[Ni(MTZ)]	IS	S	SS	SS	S

3.3 Absorption spectrum

The UV–Visible spectra of metronidazole (MTZ) and its Fe(III) and Ni(II) nano-complexes (Fig. 1) exhibit characteristic absorption bands that provide insight into the electronic transitions and coordination behavior of the ligand upon complexation.

The free metronidazole spectrum shows a prominent absorption band at $\lambda = 257$ nm ($A \approx 0.850$), which is attributed to $\pi \rightarrow \pi^*$ transitions within the nitroimidazole chromophore (Onyegbule *et al*., 2021). This band is relatively sharp and well-defined, indicating a localized electronic transition within the aromatic system. Upon coordination, this band undergoes slight shifts to ~260 nm in the Fe(III) complex and ~242 nm in the Ni(II) complex, reflecting changes in the electronic environment of the ligand. These shifts (bathochromic in Fe and hypsochromic in Ni) are indicative of metal–ligand interactions that perturb the π-electron system, consistent with coordination through the imidazole nitrogen (Refat *et al*., 2014).

In addition, a broad and intense absorption band observed at $\lambda = 323$ nm ($A \approx 2.726$) in the spectrum of free MTZ is assigned to $n \rightarrow \pi^*$ transitions associated with the non-bonding electrons of the nitro group. This band is retained in the metal complexes, appearing at 323 nm (Fe) and 326 nm (Ni), although with noticeable changes in band shape and intensity. The broadening of this band in the complexes suggests increased electronic delocalization and possible intra-ligand charge transfer contributions, arising from coordination-induced redistribution of electron density (Nakamoto, 2009; Onyegbule *et al*., 2021).

A key feature of the spectra is the change in band profile upon complexation. While the free ligand exhibits relatively sharp transitions, the metal complexes show broadened and less resolved bands, which can be attributed to (i) increased structural heterogeneity at the nanoscale, (ii) overlapping electronic transitions, (iii) and ligand field effects introduced by the metal centers. Such broadening is commonly observed in nano-coordination systems and suggests successful formation of coordination complexes with modified electronic structures.

Furthermore, the Fe(III) nano-complex displays a very weak, low-intensity absorption band at ~794 nm ($A \approx 0.02$) in the visible region. This band is assigned to a d–d transition ($^6A_1 \rightarrow {}^4T_1$) characteristic of a high-spin octahedral Fe(III) complex (Deacon & Phillips, 1980). The low intensity of this transition is consistent with its Laporte-forbidden nature. Importantly, the presence of this band provides direct spectroscopic evidence of metal coordination and confirms the formation of an octahedral Fe(III) environment (Johannes *et al*., 2023). The UV–Visible spectral (Fig. 1) results confirm that metronidazole successfully coordinates with Fe(III) and Ni(II), as evidenced by the observed shifts in absorption maxima and the emergence of metal-related transitions..

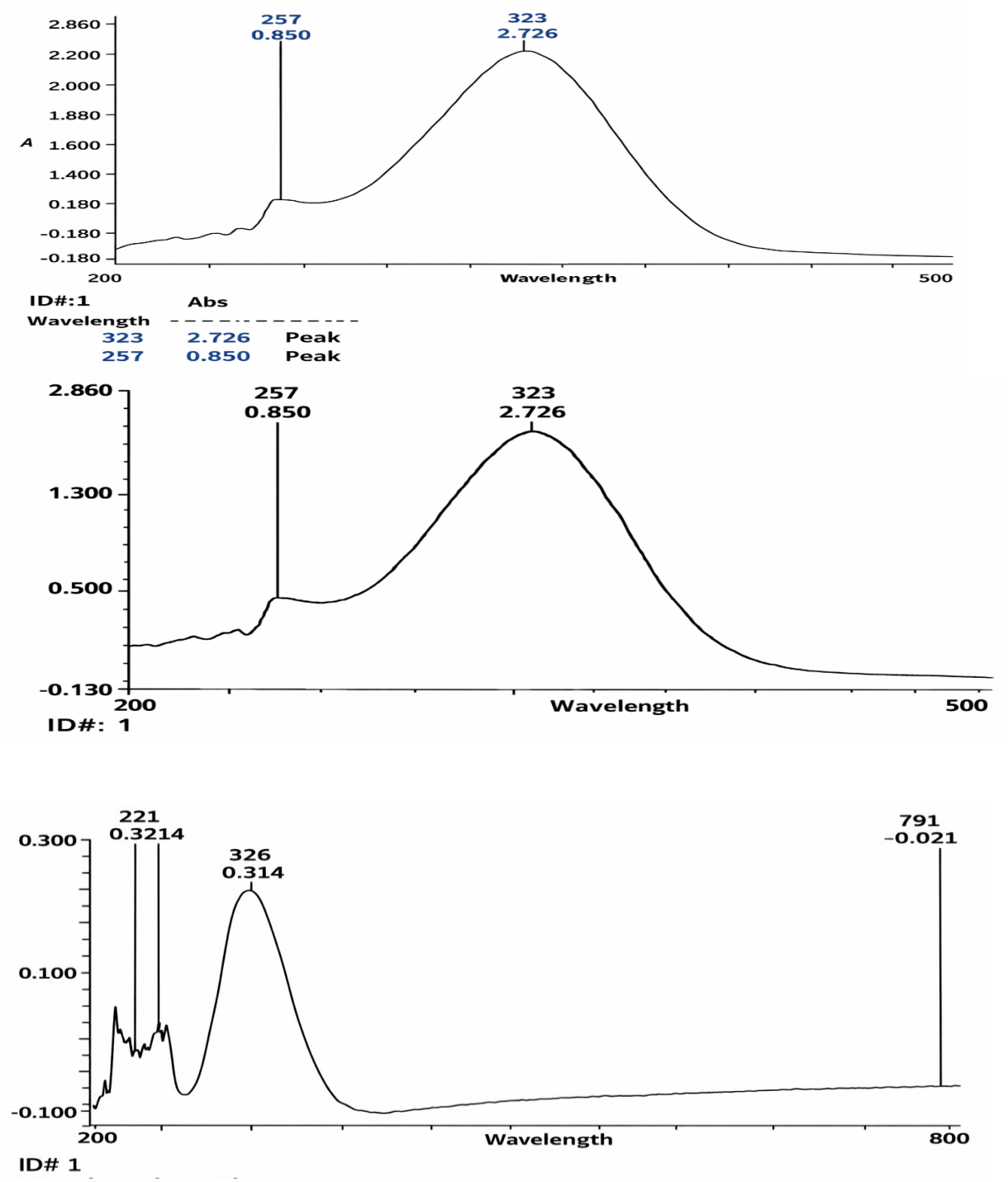

Fig. 1: UV-Visible spectra

These spectral changes indicate that coordination alters the electronic structure of the ligand, leading to redistribution of electron density within the nitroimidazole system. The broadening of absorption bands in the complexes further suggests nanoscale effects such as structural heterogeneity and overlapping transitions, supporting the formation of nano-sized coordination compounds. Additionally, the weak d–d transition observed in the Fe(III) complex provides evidence for an octahedral geometry

and high-spin configuration around the metal center. Despite these electronic modifications, the retention of the characteristic n→π* transition without significant enhancement in redox-active features supports the observed lack of antioxidant activity, indicating that metal coordination and nanosizing do not impart effective electron-donating or radical scavenging properties under the studied conditions.

3.4 Infrared Spectroscopy

The FTIR spectra of metronidazole (MTZ) and its Fe(III) and Ni(II) nano-complexes (Fig. 2) reveal significant changes in vibrational frequencies that confirm coordination and provide insight into the binding modes of the ligand. The spectrum of free metronidazole exhibits a broad absorption band at 3204 cm^{-1}, which is attributed to the O–H stretching vibration of the hydroxyl group. This band is relatively broad and intense, indicating hydrogen bonding interactions typical of free MTZ. Upon complexation, this band shifts slightly to 3190 cm^{-1} in the Ni(II) complex, accompanied by a reduction in intensity, suggesting involvement of the hydroxyl group in coordination. In contrast, the complete disappearance of this band in the Fe(III) complex indicates deprotonation of the hydroxyl group prior to coordination, implying a stronger metal–oxygen interaction in the Fe complex compared to the Ni analogue (Sadeghi & Azhdari, 2013).

This deprotonation is further supported by changes observed in the C–O stretching region, where the band shifts from 1160 cm^{-1} in free MTZ to 1150 cm^{-1} in the Fe(III) complex, reflecting a reduction in bond order due to increased electron delocalization following coordination (Zhiyong *et al*., 2016). The Ni(II) complex shows less pronounced changes in this region, indicating a comparatively weaker interaction through the oxygen donor site.

The asymmetric stretching vibration of the nitro (NO_2) group, originally observed at 1470 cm^{-1} in MTZ, undergoes notable shifts to 1490 cm^{-1} in the Fe(III) complex and 1450 cm^{-1} in the Ni(II) complex. These shifts, along with changes in band intensity and slight broadening, suggest that the nitro group participates in coordination, most likely through one of its oxygen atoms (El-Wahab *et al*., 2019). The variation in direction and magnitude of the shift between the two complexes reflects differences in metal–ligand interaction strength and electronic effects imposed by Fe(III) and Ni(II).

Furthermore, the C=N stretching vibration of the imidazole ring, appearing at 1530 cm^{-1} in free MTZ, shifts to 1521 cm^{-1} in the Fe(III) complex and 1517 cm^{-1} in the Ni(II) complex. This downward shift indicates a decrease in bond order due to coordination of the imidazole nitrogen to the metal center, confirming its role as a primary donor site. The consistent shift observed in both complexes suggests that coordination through the imidazole N_1 atom is a dominant binding mode, in agreement with established coordination behavior of imidazole-containing ligands (El-Wahab *et al*., 2019; Singh *et al*., 2012).

In addition to peak shifts, the overall spectral profiles of the complexes show band broadening and reduced resolution compared to free MTZ, particularly in the fingerprint region (1500–1000 cm^{-1}). This broadening can be attributed to increased structural complexity, overlapping vibrational modes, and nanoscale effects such as particle size distribution and surface interactions. These spectral features are consistent with the formation of nano-sized coordination complexes with altered vibrational environments.

The comparative FTIR analysis therefore confirms that metronidazole coordinates with both Fe(III) and Ni(II) through multiple donor sites, including the hydroxyl oxygen (with deprotonation in Fe), nitro oxygen, and imidazole nitrogen. The stronger spectral changes observed in the Fe(III) complex suggest a more pronounced ligand–metal

interaction relative to the Ni(II) complex. These coordination-induced modifications in vibrational frequencies and band profiles demonstrate that complexation significantly alters the electronic and structural characteristics of the ligand. However, despite these changes, the nature of the functional groups involved does not introduce strong redox-active features, which is consistent with the experimentally observed lack of antioxidant activity. The FTIR results, therefore provide critical structural evidence supporting successful complex formation while also helping to explain the limited functional enhancement in terms of antioxidant behavior.

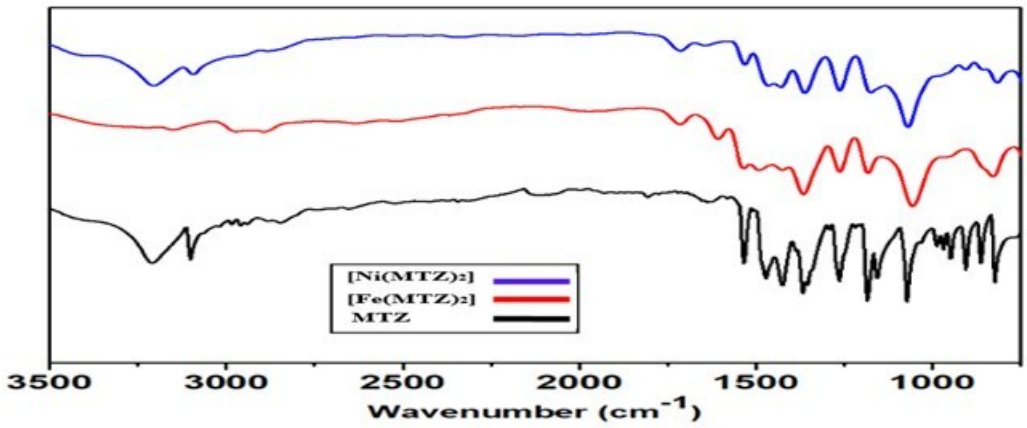

Fig 2: IR Spectra

3.5 *TEM*

Fig, 3 presents the electron micrographs of the synthesized Fe(III)–MTZ and Ni(II)–MTZ nano-complexes at different magnifications. The images (a–c) correspond to the Fe(III) complex, while (d–f) represent the Ni(II) complex. The micrographs clearly reveal the formation of nanoscale particles with distinct morphological features for both systems, confirming the effectiveness of the sonochemical synthesis route.

The Fe(III)–MTZ complex exhibits predominantly quasi-spherical to irregularly shaped particles with noticeable aggregation. The particle sizes, as indicated on the micrographs, fall largely within the range of approximately 2.70–5.32 nm, with occasional smaller nuclei (~0.52 nm) dispersed within the matrix. The particles appear closely packed, forming clustered domains, which suggests a high nucleation rate followed by limited growth. This aggregation behavior is typical of coordination-based nanomaterials, where intermolecular interactions such as hydrogen bonding and metal–ligand bridging promote particle coalescence. The relatively uniform distribution of particle sizes across different magnifications indicates a controlled nucleation process, consistent with sonochemical synthesis mechanisms involving acoustic cavitation.

In contrast, the Ni(II)–MTZ complex (Fig. 3d–f) displays a more dispersed morphology, with particles that are largely spherical but less aggregated compared to the Fe analogue. The particle sizes observed are comparable, ranging approximately from 3.22 to 5.32 nm, although the distribution appears slightly broader. The reduced degree of aggregation in the Ni complex suggests weaker interparticle interactions, which may be attributed to differences in coordination strength and electronic configuration between Ni(II) and Fe(III). Additionally, the presence of more isolated particles in the Ni system indicates improved stabilization of the nanoparticles, possibly due to differences in ligand orientation or surface charge distribution.

Comparatively, the Fe(III) complex demonstrates greater aggregation and slightly more compact nanostructures, whereas the Ni(II) complex shows better dispersion and more defined particle boundaries. These differences can be correlated with the spectroscopic results obtained earlier. The FTIR data indicated stronger coordination interactions in the Fe(III) complex, particularly involving deprotonation of the hydroxyl group, which likely enhances intermolecular bridging and leads to aggregation. Similarly, the UV–Visible spectra showed broader absorption features for the complexes, which is consistent with the structural heterogeneity and particle size distribution observed in the micrographs.

The nanoscale dimensions observed in both complexes strongly support the earlier UV–Vis findings, where band broadening was attributed to size distribution and surface effects, as well as the FTIR results indicating coordination-induced structural modification. The agreement between spectroscopic and microscopic data confirms that the synthesized materials are indeed nano-sized coordination complexes with modified electronic and structural properties.

From a technical perspective, the formation of particles within the sub-10 nm range is particularly significant, as such sizes are known to enhance surface area-to-volume ratio, dissolution rate, and potential biological interactions. The observed aggregation in the Fe(III) complex may influence its dispersibility and bioavailability, while the more dispersed Ni(II) nanoparticles may exhibit improved stability in solution. However, despite these favorable nanoscale characteristics, the lack of significant antioxidant activity observed in previous assays suggests that particle size reduction and metal coordination alone are insufficient to impart redox functionality to metronidazole. Instead, the primary implication of these findings is that the synthesized nano-complexes may be better suited for drug delivery applications, where size, morphology, and surface properties play critical roles in cellular uptake and targeted transport rather than direct antioxidant action.

Overall, the SEM/TEM analysis provides strong morphological evidence supporting successful nanoscale synthesis, complements the spectroscopic findings, and reinforces the conclusion that while structural and physicochemical properties are significantly modified, functional enhancement in terms of antioxidant activity remains limited.

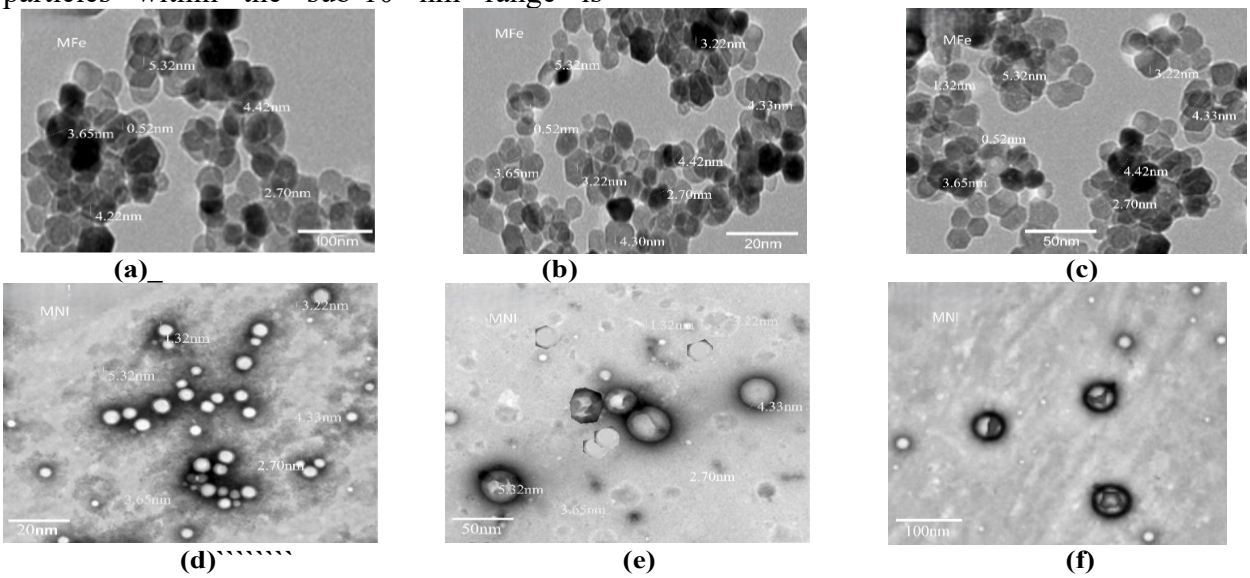

Fig 3: TEM monographs of Fe(MTZ) {a to c))] and[Ni(MTZ)](d to f)

The TEM analysis for the metronidazole-based complexes confirmed the successful formation of distinct nanoparticles. Both complexes were observed to have spherical and irregular particles, a morphology frequently observed in the co-precipitation synthesis of coordination complexes (Thanh *et al.,* 2014). The micrograph for the Fe nanocomplex of metronidazole reveals a heterogeneous and primarily nanoscale particles. The measured particle dimensions show a distribution with a significant number having sizes between 2.70 nm and 5.32 nm, alongside the presence of smaller entities around 0.52 nm. This dispersity is indicative of continuous nucleation and growth processes during synthesis. The presence of sub-3 nm particles suggests the formation of stable nuclei, while the larger particles (~5 nm) likely result from subsequent growth or a limited degree of Ostwald ripening, a process where smaller particles dissolve and re-deposit onto larger ones to minimize surface energy. The coordination of Fe^{2+} with the nitro group and imidazole nitrogen of metronidazole creates a complex that appears to self-assemble into these isotropic nanostructures, with the ligand potentially acting as a surface stabilizer, limiting uncontrolled growth (Adegoke & Ojo, 2017).

The monograph for the Ni complex of metronidazole showed a similar morphology with particle sizes recorded at 3.22 nm, 3.65 nm, 4.33 nm, and 5.32 nm. This suggests that the molecular structure of metronidazole is the primary director of nanoscale formation. The ligand's specific denticity and steric profile likely create a similar coordination environment and impose comparable kinetic barriers to crystal growth for both Fe^{2+} and Ni^{2+} ions, despite their differing electronic configurations (d^6 vs. d^8) and preferred geometries (Housecroft & Sharpe, 2018). The consistent formation of similar nano-sized particles of these metronidazole complexes is a critical finding, as particles in this sub-100 nm regime are known to exhibit enhanced cellular uptake and are prerequisite for leveraging phenomena such as the Enhanced Permeability and Retention (EPR) effect in targeted drug delivery (Patra *et al.,* 2018).

The morphological profiles of these complexes have direct consequences for the potential use of these complexes. The nanoscale of synthesized complexes makes them excellent candidates for investigation as nanomedicines. Their size is ideal for intravenous administration, potential passive targeting of diseased tissues, and improved dissolution rates (Patra *et al.,* 2018; Mitchell *et al.,* 2021).

3.6 *Proton (^{1}H) NMR*

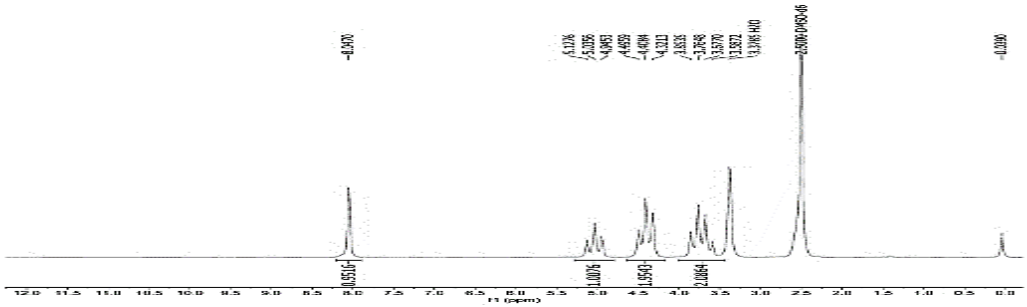

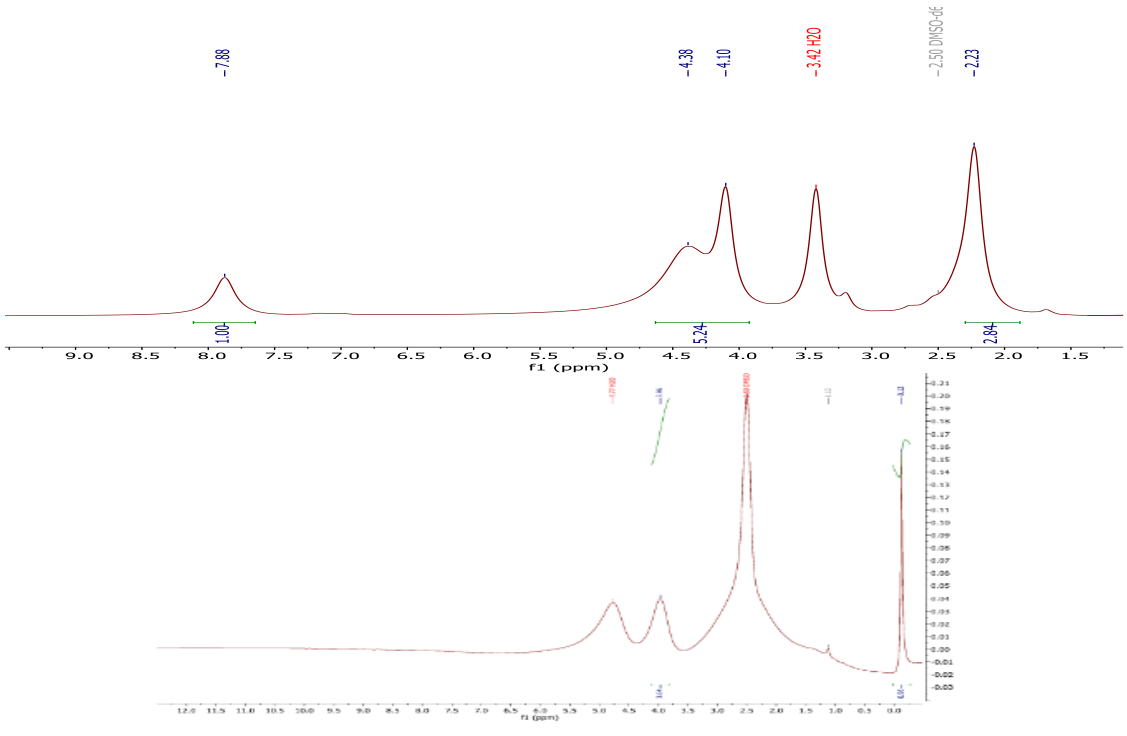

Fig 4: ^{1}H NMR of MTZ, [Fe(MTZ)$_2$] and [Ni(MTZ)$_2$]

The comparison of chemical shifts between free MTZ and its metal complexes were studied. The aromatic ring proton shows a very slight shift from 8.05 ppm in free MTZ to 7.88 and 7.95 ppm in both Fe and Ni complexes respectively. This indicates that metal coordination barely affected the electronic environment of the aromatic ring protons because the aromatic ring was not directly involved in the coordination. The OH proton observed at 5.04 ppm of MTZ shifted to 4.77 ppm in the Ni complex but was absent in the spectrum of Fe. This points to a coordination through the hydroxy oxygen with deprotonation in the Fe (III) complex (Butera *et al*., 2023; Kálmán *et al*., 2021)

The methyl protons adjacent to the imine nitrogen (H of $CH_3C=N$) show a shift from 2.46 ppm in MTZ to 2.23 and 2.50 ppm in the complexes. Even though the metal binds directly to the nitrogen, the methyl protons are only indirectly affected due to distance and shielding/deshielding interplay, causing minimal positional shift in the NMR spectrum (Butera *et al*., 2023).

All the protons for the Fe (III) complex were observed to have shifted upfield (lower ppm). This is ascribed to the paramagnetic effect of the metal center that introduces an unpaired electron spin that strongly interacts with the nuclear spins of the ligand protons resulting in large chemical shifts even when the metal is not directly bonded to the atoms (Pavel *et al.,* 2015). In contrast paramagnetic effect from the unpaired electrons on the Ni (II) metal center of a complex causes the protons to shift to downfield (higher ppm) due to the shielding effects of its own electron cloud (Mustarelli *et al.,* 2018).

Based on the spectroscopic data, the following structures have been proposed for the nano metal complexes. The DPPH assay measures the ability of a compound to donate a hydrogen atom or an electron to stabilize the purple-coloured DPPH radical, resulting in a colour change that can be measured spectrophotometrically (Mensor *et al*., 2001). A higher percentage antioxidant activity (% AA) indicates stronger free radical scavenging capability.

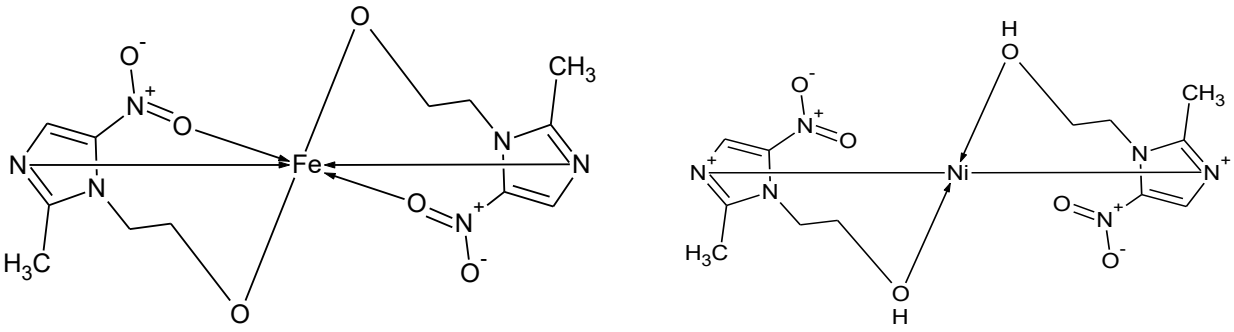

Fig: 5: Proposed structure for [Fe(MTZ)$_2$] and [Ni(MTZ)$_2$]

3.7: Antioxidant Studies

3.7.1 DPPH Result

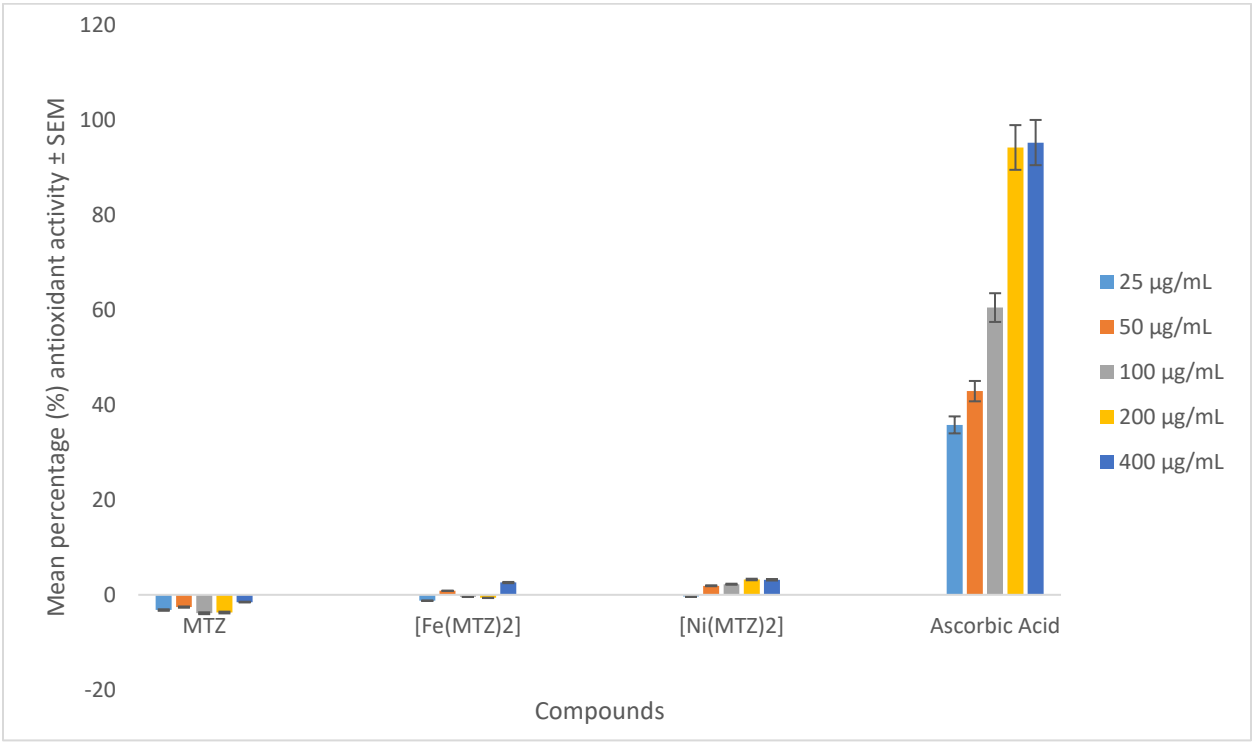

Fig 6: DPPH Result for MTZ, [Fe(MTZ)$_2$] and [Ni(MTZ)$_2$]

Metronidazole (MTZ), in its pure form, showed no appreciable DPPH scavenging activity (Fig. 6), with values hovering around or below zero. This is expected, as its nitroimidazole structure lacks readily donatable hydrogens or functional groups capable of reducing stable radicals like DPPH (Adegoke & Ojo, 2017). Both Fe (III) and Ni (II) metal complexes of MTZ failed to induce any significant radical scavenging activity. The values remained negligible or slightly negative across all tested doses when compared to that of standard (ascorbic acid) (Otuokere *et al.,* 2017). This indicates that while coordination occurs, the resulting complexes do not gain the ability to act as direct hydrogen or electron donors to the DPPH radical. The redox properties of the metal centres are either inaccessible or insufficient to overcome the inherent inertness of the metronidazole ligand in this specific assay (Otuokere *et al.,* 2025).

3.7.2 FRAP Result

The FRAP assay measures the ability of an antioxidant to reduce the ferric ion (Fe^{3+}) to the ferrous ion (Fe^{2+}) in the TPTZ complex,

producing a coloured ferrous-TPTZ complex (Benzie & Strain, 1999). It is a direct measure of electron-donating capacity (reducing power) of a compound.

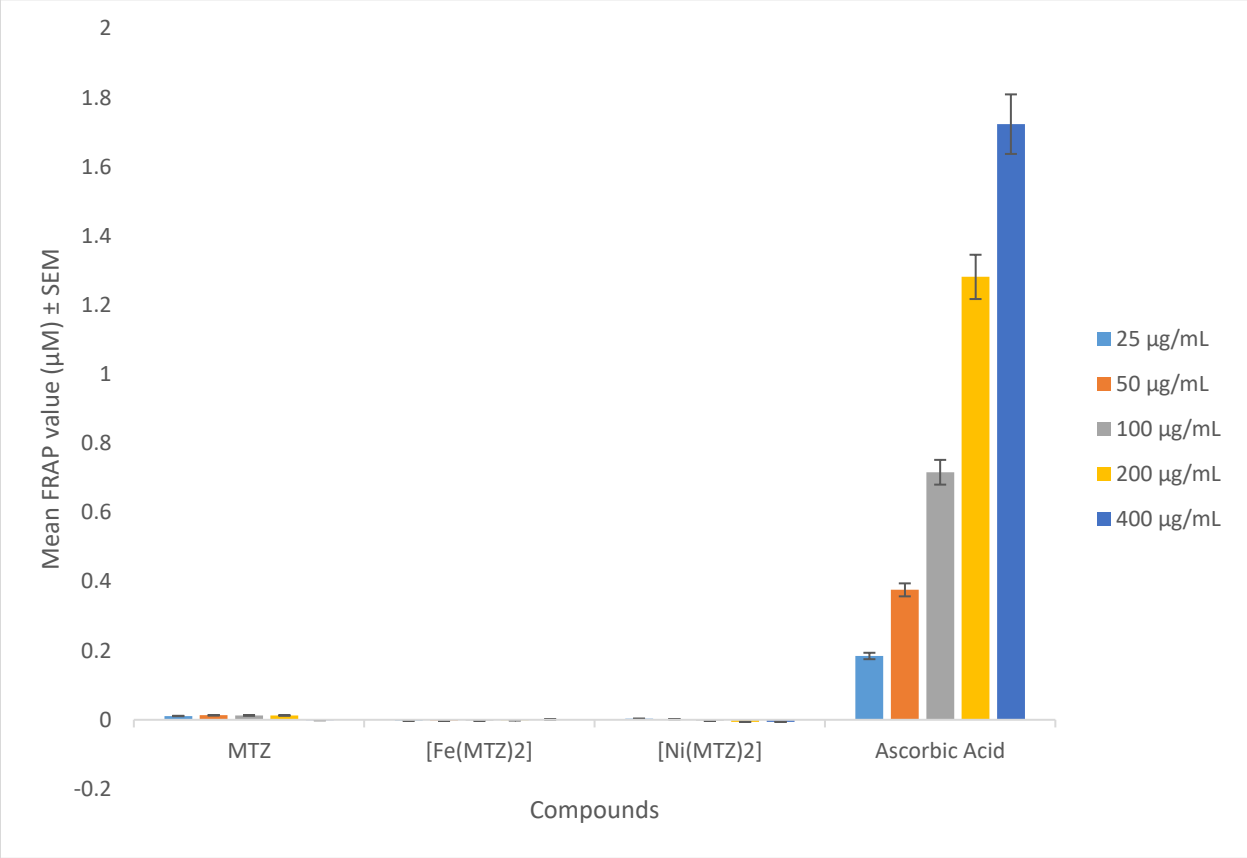

Fig 7: FRAP Result for MTZ, [Fe(MTZ)$_2$] and [Ni(MTZ)$_2$]

Metronidazole (MTZ) and its complexes (Fe (III) and Ni (II)) showed no significant ferric reducing power (Fig. 7), with absorbance values close to or below zero. This provides conclusive evidence that these compounds are not effective electron donors in this system. The lack of activity in both assays solidifies the conclusion that MTZ and its metal complexes do not function as antioxidants via hydrogen atom transfer or single electron transfer mechanisms under these conditions.

4.0 Conclusion

This study successfully reports the synthesis of nano-sized Fe(III) and Ni(II) complexes of metronidazole via a sonochemical approach, yielding stable coordination compounds with distinct physicochemical properties. Spectroscopic analyses, including UV–Visible, FTIR, and ^{1}H NMR, confirmed coordination of the ligand to the metal centers primarily through the imidazole nitrogen and hydroxyl oxygen, with evidence of deprotonation in the Fe(III) complex. The observed shifts in absorption bands and vibrational frequencies, along with changes in chemical environments, demonstrate significant modification of the electronic structure of metronidazole upon complexation.

Electron microscopy revealed the formation of predominantly spherical to irregular nanoparticles with sizes in the range of approximately 2–6 nm, confirming successful nanoscale synthesis. The Fe(III) complex exhibited slightly higher aggregation, while the Ni(II) complex showed relatively better dispersion, indicating differences in metal–ligand interaction strength and particle stabilization. These nanoscale features suggest potential advantages in terms of surface area,

dissolution, and interaction with biological systems.

Despite these structural and physicochemical modifications, antioxidant studies using DPPH and FRAP assays revealed that both metronidazole and its metal complexes possess negligible radical scavenging and reducing abilities under the conditions investigated. This indicates that metal coordination and nanosizing do not inherently impart antioxidant functionality to the ligand system.

Overall, the findings demonstrate that while Fe(III) and Ni(II) complexation significantly alters the structural and morphological properties of metronidazole, these changes do not translate into enhanced antioxidant activity. However, the nanoscale characteristics and coordination features of the synthesized complexes highlight their potential applicability in drug delivery systems and other nanomedicine-related applications, warranting further investigation into their biological and pharmacokinetic properties.

5.0 References

Adegoke, O. A., & Ojo, O. T. (2017). Metal complexation and nanoparticle synthesis of nitroimidazoles: A review. *Arabian Journal of Chemistry, 10*, S2843–S2852.

Al-Khodir, F. A. I., & Refat, M. S. (2016). Synthesis, spectroscopic, thermal and biological studies of metronidazole drug complexes with Y(III), Zr(IV), La(III) and Ce(IV). *Journal of Pharmaceutical Sciences and Research, 8*(7), 655–664.

Asogwa, B. C., & Otuokere, I. E. (2024). Sonochemical synthesis and characterization of Fe(II) and Cu(II) nano-sized complexes of sulfamethoxazole. *Journal of the Nigerian Society of Physical Sciences, 6*, 2011. https://doi.org/10.46481/jnsps.2024.2011

Asogwa, B. C., Etim, G. I., Otuokere, I. E., & Amadi, K. O. (2025). Synthesis, characterization and in-silico study of Mn(II) and Zn(II) nano-sized complexes of metronidazole synthesized via sonication method. *Communication in Physical Sciences, 12*(8), 2280–2299.

Asogwa, B. C., Mac-Kalunta, O. M., Iheanyichukwu, J. I., Otuokere, I. E., & Nnochirionye, K. (2024). Sonochemical synthesis, characterization and ADMET studies of Fe(II) and Cu(II) nano-sized complexes of trimethoprim. *Journal of the Nigerian Society of Physical Sciences, 6*, 2048. https://doi.org/10.46481/jnsps.2024.2048

Asogwa, B. C., Nyah, N. U., Otuokere, I. E., Igwe, O. U., & Amadi, K. O. (2025). Synthesis, characterization, antibacterial activity of 2-hydroxy benzylideneamino benzenesulfonamide Schiff base and its Co(II) and Ni(II) complexes. *Communication in Physical Sciences, 12*(8), 2199–2211.

Benzie, I. F., & Strain, J. J. (1999). Ferric reducing/antioxidant power assay: Direct measure of total antioxidant activity of biological fluids and modified version for simultaneous measurement of total antioxidant power and ascorbic acid concentration. *Methods in Enzymology, 299*, 15–27.

Butera, R., & Clegg, J. K. (2023). NMR spectroscopy in the analysis of paramagnetic metal complexes. *Annual Reports on NMR Spectroscopy, 98*, 1–50.

Deacon, G. B., & Phillips, R. J. (1980). Relationships between the carbon–oxygen stretching frequencies of carboxylate complexes and the type of carboxylate coordination. *Coordination Chemistry Reviews, 33*, 227–250.

El-Wahab, H. A., Atta, M., Hassan, W. A., & Nasser, A. M. (2019). Preparation, characterization and evaluation of some acrylate polymer nanoparticles as binders for improving the physical properties of water-based paints. *International Journal of Nanoparticles and Nanotechnology, 5*, 022.

Housecroft, C. E., & Sharpe, A. G. (2018). *Inorganic chemistry* (5th ed.). Pearson.

Iwalewa, E. O., Adewale, I. O., Aiwo, B. J., Arogundabe, T., Osinowo, A., Daniyan, O. M., & Adetogun, G. E. (2008). Effects of *Harungana madagascariensis* stem bark extract on antioxidant markers in alloxan-induced diabetic and carrageenan-induced inflammatory disorders in rats. *Journal of Complementary and Integrative Medicine, 5*(1), 1–18.

Johanness, P. T., Henning, M. K., & Nico, M. (2023). UV–Vis spectrophotometric analytical technique for monitoring Fe^{2+} in the positive electrolyte of an ICRFB. *Journal of Power Sources, 553*, 232178.

Kálmán, F. K., & Tircsó, G. (2021). NMR studies of paramagnetic metal complexes for MRI applications. *Contrast Media & Molecular Imaging, 2021*, 6644978.

Löfmark, S., Edlund, C., & Nord, C. E. (2010). Metronidazole is still the drug of choice for treatment of anaerobic infections. *Clinical Infectious Diseases, 50*(Suppl. 1), S16–S23.

Mensor, L. L., Menezes, F. S., Leitão, G. G., Reis, A. S., dos Santos, T. C., Coube, C. S., & Leitão, S. G. (2001). Screening of Brazilian plant extracts for antioxidant activity using the DPPH free radical method. *Phytotherapy Research, 15*(2), 127–130.

Mitchell, M. J., Billingsley, M. M., Haley, R. M., Wechsler, M. E., Peppas, N. A., & Langer, R. (2021). Engineering precision nanoparticles for drug delivery. *Nature Reviews Drug Discovery, 20*(2), 101–124.

Mustarelli, P., & Grandinetti, F. (2018). Paramagnetic solid-state NMR and polymorphism in transition-metal oxides. *The Journal of Physical Chemistry Letters, 9*(20), 6072–6076.

Nakamoto, K. (2009). *Infrared and Raman spectra of inorganic and coordination compounds* (6th ed., Part B). Wiley.

Nyah, N. U., Asogwa, B. C., Otuokere, I. E., Igwe, O. U., & Amadi, K. O. (2025). Synthesis, characterization, antibacterial activity of 2-hydroxy benzylideneamino benzenesulfonamide Schiff base and its Co(II) and Ni(II) complexes. *Communication in Physical Sciences, 12*(8), 2199–2211.

Nyah, N. U., Asogwa, B. C., Otuokere, I. E., Igwe, O. U., & Amadi, K. O. (2026). Synthesis, characterization, antibacterial activity of 2-hydroxy benzylideneamino benzenesulfonamide Schiff base and its Fe(II) and Cu(II) complexes. *Applied Sciences, Computing and Energy, 4*(1), 48–64.

Onyegbule, F. A., & Udeozo, I. P. (2021). Spectral and antimicrobial properties of metal complexes of metronidazole. *International Journal of Scientific Research in Chemical Sciences, 8*(2), 10–17.

Otuokere, I. E., Ohwimu, J. G., Amadi, K. C., Alisa, C. O., Nwadire, F. C., Igwe, O. U., Okeyeagu, A. A., & Ngwu, C. M. (2019). Synthesis, characterization and molecular docking studies of Mn(II) complex of sulfathiazole. *Journal of the Nigerian Society of Physical Sciences, 1*(3), 95–102.

Otuokere, I. E., Okorie, D. O., Asogwa, B. C., Amadi, O. K., Ubani, L. O. C., & Nwadire, F. C. (2017). Spectroscopic and coordination behavior of ascorbic acid towards copper(II) ion. *Research in Analytical and Bioanalytical Chemistry, 1*(1), 1–7.

Otuokere, I. E., Iheanyichukwu, J. I., Asogwa, B. C., Mac-Kalunta, O. M., et al. (2025). GC–MS, antioxidant, anti-inflammatory and in-silico studies of a polyherbal formulation. *Discovery Chemistry, 2*, 121.

Pallavi, P., & Singh, R. (2025). Solubility and dissolution enhancement of poorly soluble drugs via metal complexation. *Journal of Pharmaceutical Innovation, 20*(1), 123–135.

Patra, J. K., Das, G., Fraceto, L. F., Campos, E. V. R., Rodriguez-Torres, M. D. P., Acosta-Torres, L. S., & Shin, H. S. (2018). Nano-based drug delivery systems: Recent developments and future prospects. *Journal of Nanobiotechnology, 16*(1), 71.

Pavel, B. T., Jordan, M. C., Jason, B. B., & Janet, R. M. (2015). Six-coordinate iron(II) and cobalt(II) parashift agents for temperature measurement by magnetic resonance spectroscopy. *Inorganic Chemistry, 55*(2), 700–716.

Refat, M. S., El-Korashy, S. A., & Ahmed, A. S. (2014). Synthesis and characterization of metronidazole complexes with Mg(II), Ca(II), Sr(II) and Ba(II). *Journal of Molecular Structure, 1062*, 155–163.

Sadeghi, M., & Azhdari, T. (2013). Synthesis and characterization of metronidazole complexes with transition metals and their antimicrobial activity. *Journal of Coordination Chemistry, 66*(14), 2495–2505.

Singh, N. K., Singh, S. B., & Muthu, S. (2012). Synthesis, characterization, and biological activities of some metal complexes of metronidazole. *Journal of Coordination Chemistry, 65*(8), 1319–1330.

Thanh, N. T. K., Maclean, N., & Mahiddine, S. (2014). Mechanisms of nucleation and growth of nanoparticles in solution. *Chemical Reviews, 114*(15), 7610–7630.

Zhiyong, L., Van Kien, L., Malini, O., & Weng, K. L. (2016). Vibrational spectroscopy of metal carbonyls for bio-imaging and sensing. *Analyst, 141*(5), 1569–1586.

Declaration

Funding sources

No funding

Competing Statement

There are no competing financial interests in this research work.

Ethical considerations

Not applicable

Data availability

The microcontroller source code and any other information can be obtained from the corresponding author via email.

Authors' Contribution

Okezie C. carried out the experimental work. Brendan C. Asogwa interpreted the results, drafted the initial manuscript. Ifeanyi E. Otuokere conceptualized and supervised the study, led in result interpretation and reviewed the manuscript. Mbara C. assisted in the carrying out the laboratory work. Ubani L. O. C. supervised the lab work and assisted in reviewing the manuscripts.